AIAA SPACE Forum
17-19 September 2018, Orlando, FL
2018 AIAA SPACE and Astronautics Forum and Exposition

10.2514/6.2018-5185

Geometry and Structural Stability of Lunar Lava Tubes

A. K. Theinat[1] and A. Modiriasari[2]
Graduate Student[1], Lyles School of Civil Engineering, Purdue University, West Lafayette, Indiana, 47907, USA.
Post-Doctoral Researcher[2], Lyles School of Civil Engineering, Purdue University, West Lafayette, Indiana, 47907, USA.

A. Bobet
Professor, Lyles School of Civil Engineering, Purdue University, West Lafayette, Indiana, 47907, USA.

H. J. Melosh
Professor, Department of Earth, Atmospheric, and Planetary Sciences, Purdue University, West Lafayette, Indiana, 47907, USA.

S. J. Dyke
Professor, Lyles School of Civil Engineering and Department of Mechanical Engineering, Purdue University, West Lafayette, Indiana, 47907, USA.

J. Ramirez
Professor, Lyles School of Civil Engineering, Purdue University, West Lafayette, Indiana, 47907, USA.

A. Maghareh
Post-Doctoral Researcher, Lyles School of Civil Engineering, Purdue University, West Lafayette, Indiana, 47907, USA.

D. Gomez
Graduate Student, Lyles School of Civil Engineering, Purdue University, West Lafayette, Indiana, 47907, USA.

[Abstract] Establishment of extraterrestrial habitats on other planets is of interest to research and industry. Underground habitats, given that they are not exposed to extreme hazards such as radiation, meteorite impacts, and temperature fluctuations, can potentially serve as secure shelters for future human exploration. Images and measurements from SELENE and LRO support the presence of natural openings on the Moon. Data from GRAIL also investigated the possibility of the existence of large empty tunnels (1-2 km wide) in the lunar lava flows. Those tunnels could have been created when a crust formed on top of the lava flows. Using the characteristics and the morphology of the lava flows, an analytical solution has been developed to estimate the size of the lunar lava tubes. Also, a series of numerical simulations has been conducted to investigate the stability of the lava tubes for different sizes and material properties. The numerical solutions provide a more refined approach than previous attempts at investigating the stability of the lunar lava tubes. The results show that stability is influenced by the roof thickness and rock properties, particularly the tensile strength of the solid lava. Both analytical and numerical simulations show that the existence and stability of lunar lava tubes with widths of 1 km or more is possible, which agrees with the GRAIL observations. Also, the study shows that the tensile strength of the rock mass is a crucial parameter for stability assessment. For any particular width and height of the lava tubes, lower tensile strengths of the rock necessitate larger roof thicknesses for the lava tubes to remain stable.

Nomenclature

Q_E = Effusion rate
κ = Thermal diffusivity of the lava in the flow

G_z = Gratz number
Y_B = Bingham yield stress of the lava
ρ = Density of the lava
g = Acceleration of gravity
A = Area of the lava flow
θ = Average slope of the surface on which lava is flowing
V = Average velocity of the lava flow
T_o = Maximum tensile strength of the rock based on the Mohr-Coulomb failure envelope
T = Tensile strength of the rock assumed in the analysis.
h/H = Percentage of the plastic yielding in the crown relative to the total roof thickness

I. Introduction

Extraterrestrial habitats could provide shelter to future astronauts and serve as outposts for manned missions to other planets. Those habitats should be designed to be resilient and safe under different hazards conditions [1, 2]. Subsurface habitats are attractive as they are safer from hazards such as radiation and meteorite impacts than habitats on the surface. There is evidence of the existence of natural underground structures on the Moon, in the form of large lava tubes, that could be used for permanent human habitats. The basaltic roof of those underground openings may protect from cosmic radiation, meteorite impacts, and the extreme diurnal temperature variations [3, 4]. Lava tubes could potentially be used as natural storage facilities as they are large and may need little construction effort. Nearby volcanoes could provide geological materials, such as sulfur, iron and oxygen [5]. Drilling in lava tubes may also provide for the expansion of the cave network and the extraction of underground resources [5].

Those naturally occurring tubes may be formed by crusting over the still-molten lava flowing under the surface. The opening is formed after the lava drains and the crust cools down [6]. Lava tubes on the Moon seem to have larger sizes than terrestrial or Martian lava tubes. The sizes of tubes on Earth vary from 10-30 m [7, 8], on Mars from 250-400 m [8], and the presence of lava tubes with few kilometers width might be possible on the Moon [8]. The existence of lunar lava tubes has been investigated using images taken from skylights (holes into the tubes) and gravity data analysis. The first image was taken in 2009 by SELenological and ENgineering Explorer (SELENE) spacecraft which showed a vertical hole with a diameter of 65 m. In addition, 150 pits were observed by the Lunar Reconnaissance Orbiter (LRO) with an estimated roof thickness of ~75 m and widths of 49-106 m [9-11]. Later on, the Gravity Recovery And Interior Laboratory (GRAIL) used the gravity data to characterize subsurface density variations using eigenvalue mapping and cross-correlation between gravity signals and the assumed lava tubes features. The width of the lava tubes was initially estimated as 1-2 km from the mass deficits estimated from GRAIL's gravity data [12-17].

The primary concern regarding those large openings is their stability. Oberbeck et al. (1969) used the single beam theory to estimate the possible width of lava tubes that was necessary to maintain stability [18]. A 65 m beam depth (roof thickness) was used in the analysis, which was estimated based on the shadow measurement of Rille A at the Marius Hill Hole. A maximum possible width of 385 m was estimated in the study, assuming a lunar basalt density of 2,500 kg/m^3. However, arching mechanisms and differential stresses (initial state of stress) were ignored in the analysis, which could have resulted in underestimating the maximum possible width [9, 18]. Blair et al. (2017) conducted numerical analyses on lava tubes with different roof thicknesses [19]. In the analyses, they assumed a horizontal ellipse, as the cross-section, with a height to width ratio of 1:3. They concluded that, for a 2 m roof thickness, the lava tubes could remain stable with a width of 1 km or more. The studies showed that the basaltic roof thickness was a crucial parameter for the stability of the lava tubes.

The size, geometry and the structural stability of the lunar lava tubes are still not fully understood and need further research. In this paper, analytical solutions are used to estimate the size of the lava tubes based on the lava flow characteristics and the lunar topography. Viscous lava with Bingham rheology is assumed. In addition, numerical simulations are presented to determine the structural stability of the lava tubes for different roof thicknesses and material properties. The simulations are based on a finite element approach implemented through ABAQUS© [20]. The material properties are assessed using the Geological Strength Index (GSI). The results from the analytical and numerical solutions are compared with data from GRAIL and other observations to better understand the formation and stability of lunar lava tubes.

II. Geometry of Lava Tubes

The existence of the lava tubes at sizes comparable to those inferred from the GRAIL data is analyzed using knowledge of lunar rocks and the mechanics of lava flows. The extent of a lava tube is affected by the effusion rate of lava from a feeder vent and how magma is transported beneath the surface. The effusion rate (Q_E) depends on the eruption rate, which cannot be measured directly from past eruptions. A method of estimating the effusion rate is through the ratio between the heat advected during flow and the heat conducted (the Gratz number (G_z)) [22]. The effusion rate of a single lava flow on a surface with average slope θ can be obtained as [22]:

$$Q_E = \frac{\kappa\, A\, G_z}{Y_B} \rho g sin\theta$$

where κ is the thermal diffusivity of the lava composing the flow, A is the area of the lava flow, Y_B is the Bingham yield stress of the lava flow, ρ is the density of the lava, and g is the acceleration of gravity.

The parameters used in the analytical solution are shown in Table 1. As a result, the effusion rate is estimated to be up to 2×10^6 m^3/s (note that here we try to assess the largest possible size of lava tubes). Subsequently, the cross-section area of the lava tubes can be estimated as $7\times 10^5 - 1 \times 10^6$ m^2 for an average velocity of the lava flow of ~1.5-3 m/s.

Table 1. Geometry and material properties of lunar lava flows.

Parameter	Value
Thermal diffusivity; κ	10^{-6} m^2/s [22]
Density; ρ	2,790 kg/m^3 [22]
Gratz number; G_z	30 [22]
Bingham yield stress; Y_B	3.8-59,151 Pa [23]
Area of flow; A	0.3-2,434 (km^2) [24]
Slope; θ	0.01-1.4 (degree) [24]
Velocity of flow; V	1.5-3 m/s [25]

Lava tubes can have different shapes. If the cross section is circular or elliptical (with a width to height ratio of 3:1 or 1:3), the resulting width of the tube is around 1 km (assuming that the tube runs full). This is comparable to the data reported by GRAIL [26].

III. Structural Stability of Lava Tubes

The structural stability of lunar lava tubes is investigated through numerical modeling. Simulations are conducted for different geometry configurations and tensile strengths of the rock mass, as shown in Fig. 1 and Table 2. A 1,000 m width lava tube is modelled, according to the results from GRAIL and the analytical solution. In addition, a larger tube size, of 4,000 m width, is also analyzed because this is one of the largest sizes that might be stable according to the analysis of Blair et al. (2017) [19].

The height of the lava tube opening is one-third of the width, i.e. 333 m and 1,333 m for the 1,000 m and 4,000 m wide tubes, respectively. The 1:3 ratio is chosen as representative of the lava tubes found on Earth [19]. Different roof thicknesses are investigated, ranging from 20 m to 2,000 m.

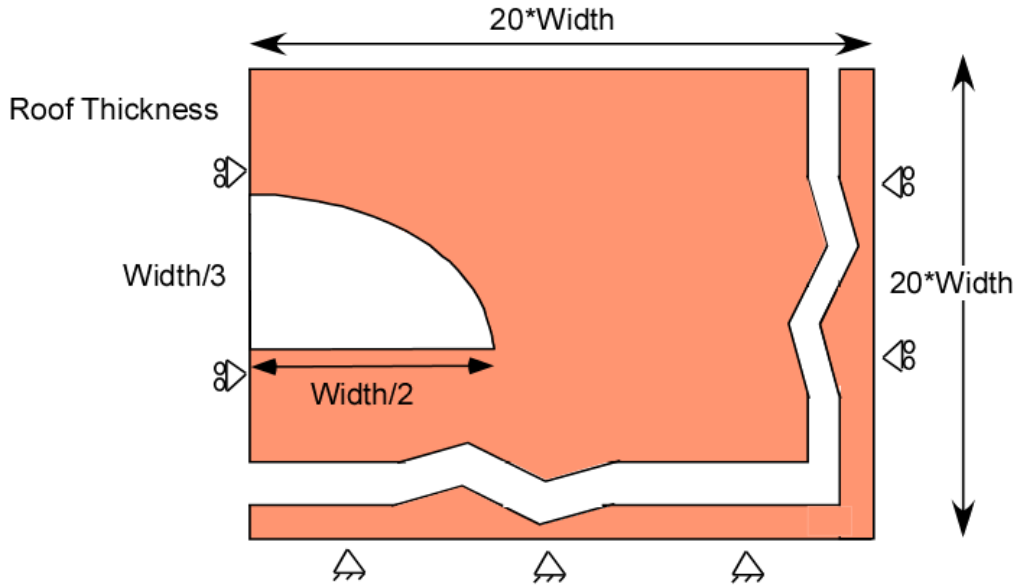

Fig.1. Model setup.

Table 2. Geometry and tensile strength used in the model.

Width (m)	Height (m) = Width/3	Roof thicknesses (m)	Tensile strength (% of the compressive strength)
1,000	333	20 - 2,000	100% - 0.8%
4,000	1,333	20 - 2,000	100% - 0.2%

A. Modelling Techniques

The analyses are conducted using ABAQUS© [20]. It is assumed that the length of the lava tube is much larger than the size of its cross section, and so plane strain conditions apply to any cross-section perpendicular to the axis of the tube. Due to symmetry, only half of the cross section is simulated. As shown in Fig. 1, the boundaries are placed far from the opening (20 times the tube width) to minimize their effect on the results. The sides of the model are constrained in the horizontal direction while the bottom boundary is constrained in both vertical and horizontal directions. Six-nodes continuum plain strain elements (CPE6) are used for the mesh shown in Fig.2.

Loading is applied by imposing gravity. Note that horizontal stresses are induced because no horizontal displacements are allowed at the lateral boundaries of the model. An elastic-perfectly plastic constitutive model for the material is assumed, with a Mohr-Coulomb failure criterion. The material parameters are estimated based on the Geological Strength Index (GSI). This index evaluates the strength and properties of the rock mass using a description of the rock mass structure and the type of rock [27].

It is assumed that the GSI has an average value of 70, based on the visual examination of images of lava tubes at different locations on Earth such as Hawaii, California, Washington, and Oregon, in the USA, in Iceland, Spain, Kenya, Portugal, and South Korea. Based on Hoek and Brown (2004) [27], a GSI=70 and UCS (Unconfined Compression Strength) of 100 MPa (from a range of 100-250 MPa for basaltic rock [27]), the material properties of the rock mass around the lava tubes are obtained and are listed in Table 3. The density of the basaltic rock is taken as 3,100 kg/m^3, after Kiefer et al. (2012), from samples of lunar basaltic rocks [28].

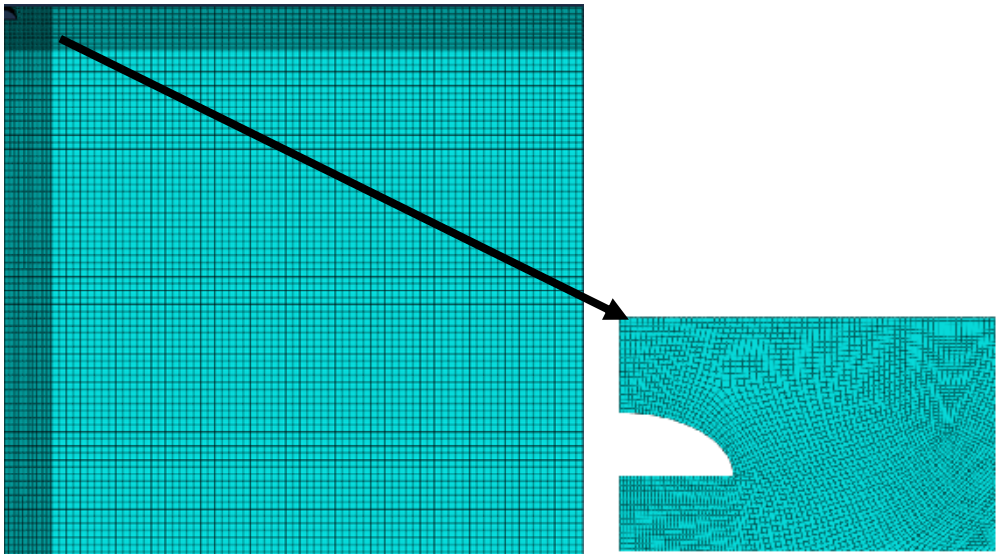

Fig.2. Mesh configuration.

Table 3. Material properties used in the model.

Geological Strength Index	70
Density (kg/m^3)	3100 [28]
Stiffness (GPa), Poisson's Ratio	30, 0.3 [27]
Cohesion (MPa)	7.2 [27]
Friction Angle (°), Dilation Angle (°)	43, 29 [27]
Unconfined Compressive Strength (MPa)	32 [27]
Tensile Strength (MPa)	0.52-1.3 [27]
Tensile / Compressive Strength (%)	1.7-4.3

The stress-strain diagram as well as the Mohr-Coulomb failure envelope are shown in Figs. 3a and 3b. Yielding in compression is denoted as σy_c while in tension, σy_t. Rock has limited tensile capacity, in particular when it is fractured, which is expected given the formation of the lava tubes through cooling.

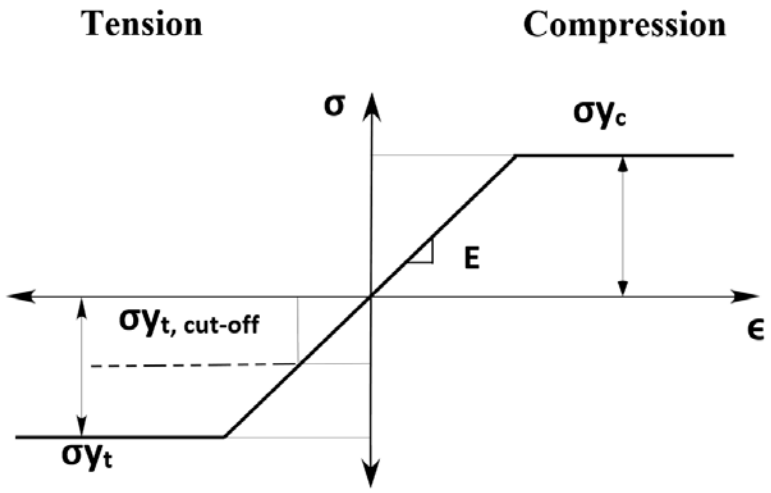

(a)

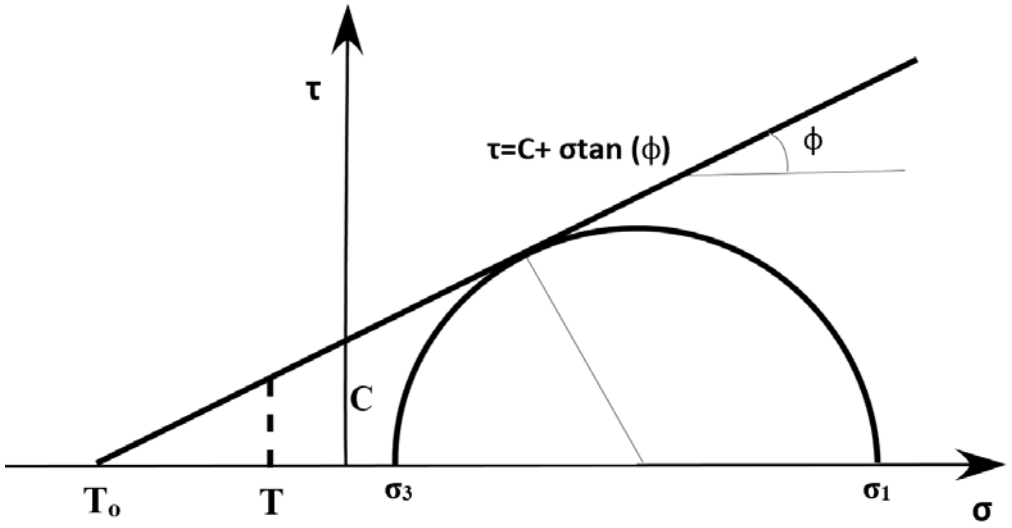

(b)

Fig.3. Tension cut-off in the Mohr-Coulomb failure criterion shown in: (a) the stress-strain diagram; (b) Mohr-Coulomb failure envelope.

The tensile strength of the rock in the Mohr-Coulomb failure criterion, T_o, can be calculated based on the friction angle (ϕ), and the cohesion (C) in Figs. 3a and 3b. To account for a weaker material in tension, e.g. due to fracturing, a tension cut-off is implemented ($\sigma y_{t,\text{ cut-off}}$ or T in Figs. 3a and 3b, respectively), which can be as low as 0.2% to 0.8% of the UCS (Table 2).

B. Simulations Results

The stability of lava tubes can be evaluated using the height of rock yielding above the crown, as suggested by Blair et al., (2017) [19]. As shown in Fig. 4, the stability is defined using the height of plastic yielding above the crown relative to the roof thickness; h/H (%).

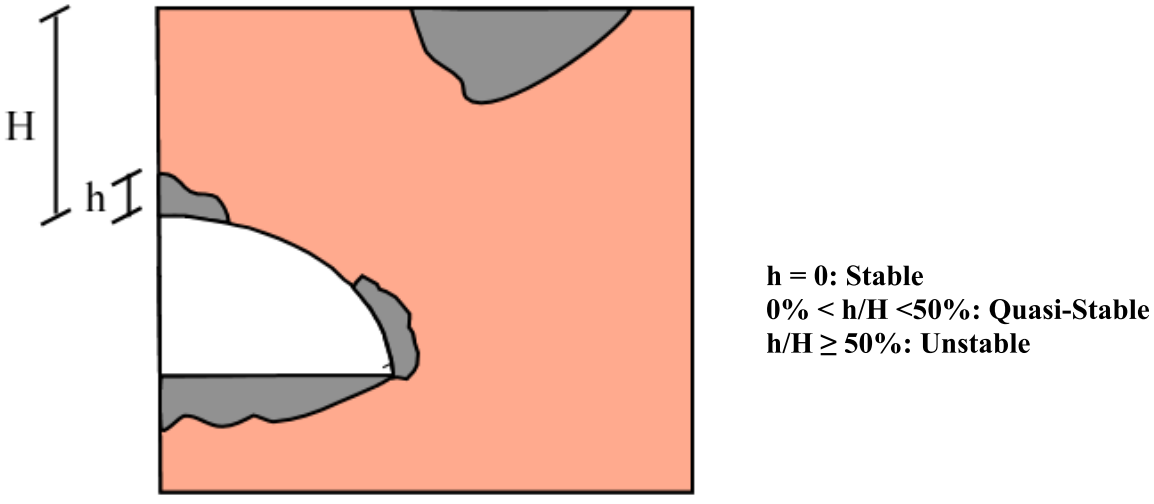

Fig.4. Stability defined by the percentage of rock yielding above the crown (h) relative to the roof thickness (H).

The influence of roof thickness on the stability of the opening is investigated through a limited parametric analysis where different thickness, ranging from 20 m to 2,000 m are investigated. All the simulations are done with the full tensile strength of the rock mass, T_o. Fig. 5 is a plot of the size of the overburden yielding, defined by the ratio h/H in Fig.4.

The results for the opening with the 1,000 m width showed no yielding even for the smallest overburden, which is supported by the results from Blair et al., 2017 [19]. This suggests that widths of 1,000 m, which are consistent with observations from GRAIL, should be stable for roof thicknesses as low as 20 m (all other factors being equal). This is not the case when the tube is 4,000 m wide. For a roof thicknesses from ~100 to 2,000 m, the percentage yielding (h/H~10%) is fairly uniform and small, so the lava tube can be considered quasi-stable using the criterion in Fig. 4. As the roof thickness decreases below about 100 m, the amount of rock yielding increases quickly. Below 30 m, yielding increases significantly (h/H>50%), which denotes a strong potential for failure.

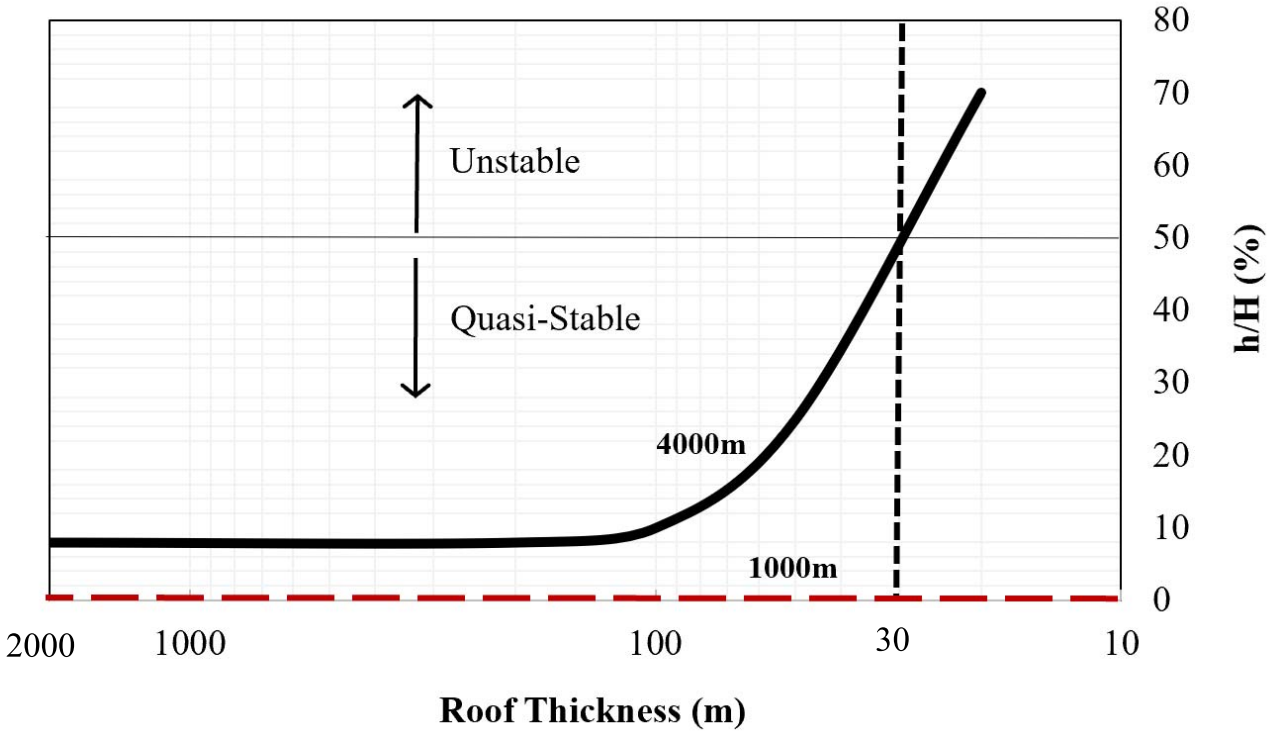

Fig.5. Plastic yielding of the overburden for different tube widths and roof thicknesses.

It is questionable that the rock mass will be able to develop the full tensile capacity T_o given by the Mohr-Coulomb failure (Fig. 3). Rather, a fraction of the tensile strength will be available due to the presence of tensile fractures (likely due to cooling of the lava and possible due to tectonic stresses). To study the influence of the tension cut-off on the stability, a parametric analysis is attempted. The two cases, with widths of 1,000 m and 4,000 m, are used in the simulations. The thickness of the overburden is kept constant to half the width of the opening; that is, to 500 m and 2,000 m, respectively.

The results of the numerical simulations are plotted in Fig. 6. Fig. 6a shows that there is no yielding for the 1,000 m wide tunnel until the tension cut-off is reduced to about 2.5% of the UCS. After that, yielding of the rock above the crown increases dramatically. Fig. 6b shows the results for the 4,000 m wide tunnel. There is some yielding, about 15% of the overburden, up to T/UCS of about 5%. Afterwards, the volume of yielding of the overburden increases very quickly.

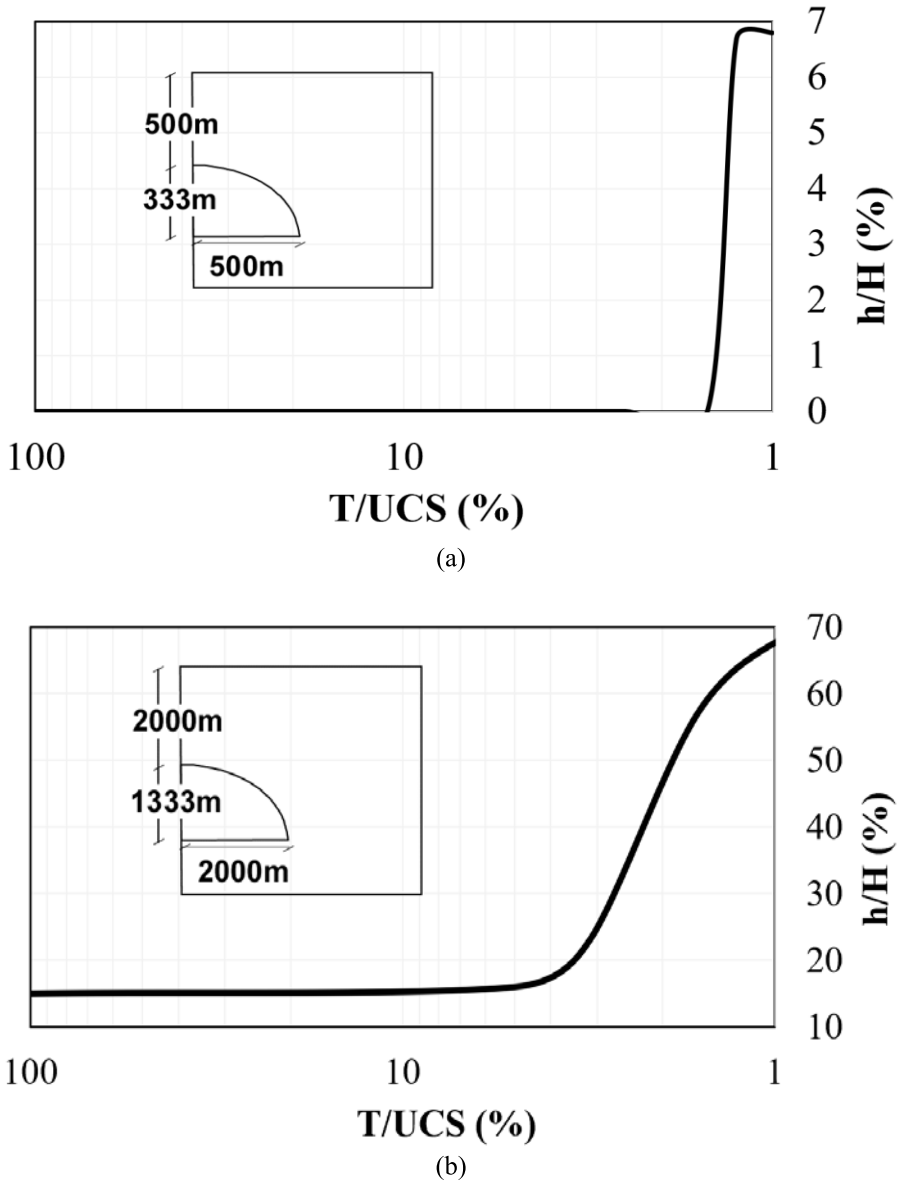

Fig. 6. Yielding of the crown (% of roof thickness) with respect to tension cut-off for widths of a) 1,000 m, and b) 4,000 m.

Fig. 7 shows the volumes or rock that yield around the tunnel for the case of 4,000 m opening width and 2,000 m overburden. A solid color is used for results with no tension cut-off, and dashed pattern when T/UCS is 0.8%. Yielding increases as the tensile strength capacity of the rock decreases. As one can see, yielding not only occurs above the crown, but also below the invert and below the surface, far from the tunnel. This denotes a more complex response than that estimated by Blair et al. (2017), and thus the stability criterion may not be as straightforward as previously assumed. Thus, the volume of rock yielding may or may not represent the degree of stability of an underground structure. We use tunnel convergence as the stability criterion, which is defined as the difference of radial displacements between two points located on the perimeter of the tunnel that are diametrically opposed. The two points used in this study are shown in Fig. 8, and are located at the crown and invert along a vertical line through the center of the tunnel. Convergence measurements are routinely used in tunnel construction and tunnel engineering to monitor the response of the tunnel to excavation, loading, etc. and to assess the stability of the tunnel.

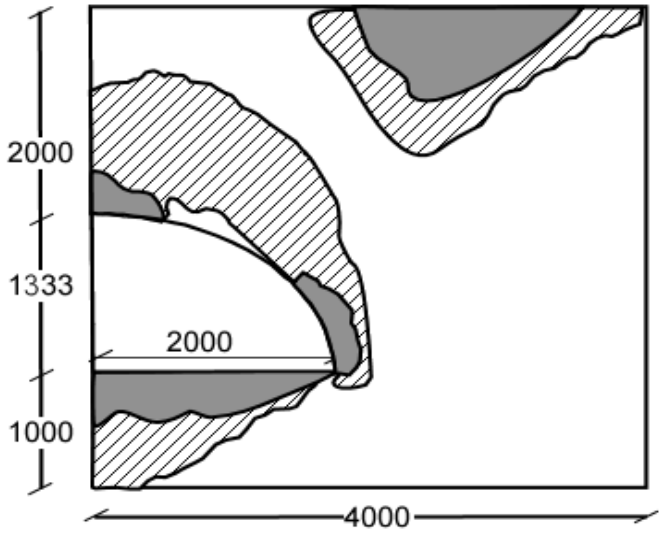

Fig.7. Plastic yielding for a 4,000 m wide lava tube and 2,000 m roof thickness (solid color represents results with no tension cut-off, while dashed pattern for tension cut-off T/UCS ~0.8%). All dimensions are in meters.

Fig. 8 shows the results of the tunnel convergence for the case of the lava tube with a width of 1,000 m and overburden thickness of 500 m, for different values of the tension cut-off. As one can see, the values are quite small even for small values of the tension cut-off. Overall, the results indicate stability of the opening. Fig. 9 is an analogous plot, but for the case of the opening with 4,000 m width and 2,000 m overburden. The figure shows that convergence is small up to T/UCS of 1%; then, it increases slowly as the tensile strength reduces up to T/UCS of about 0.2%; after that, the tunnel deformations increase very quickly. Given that the estimated values of the rock mass tensile strength may range from 1.7% to 4.3% (Table 3), the opening can be classified as stable.

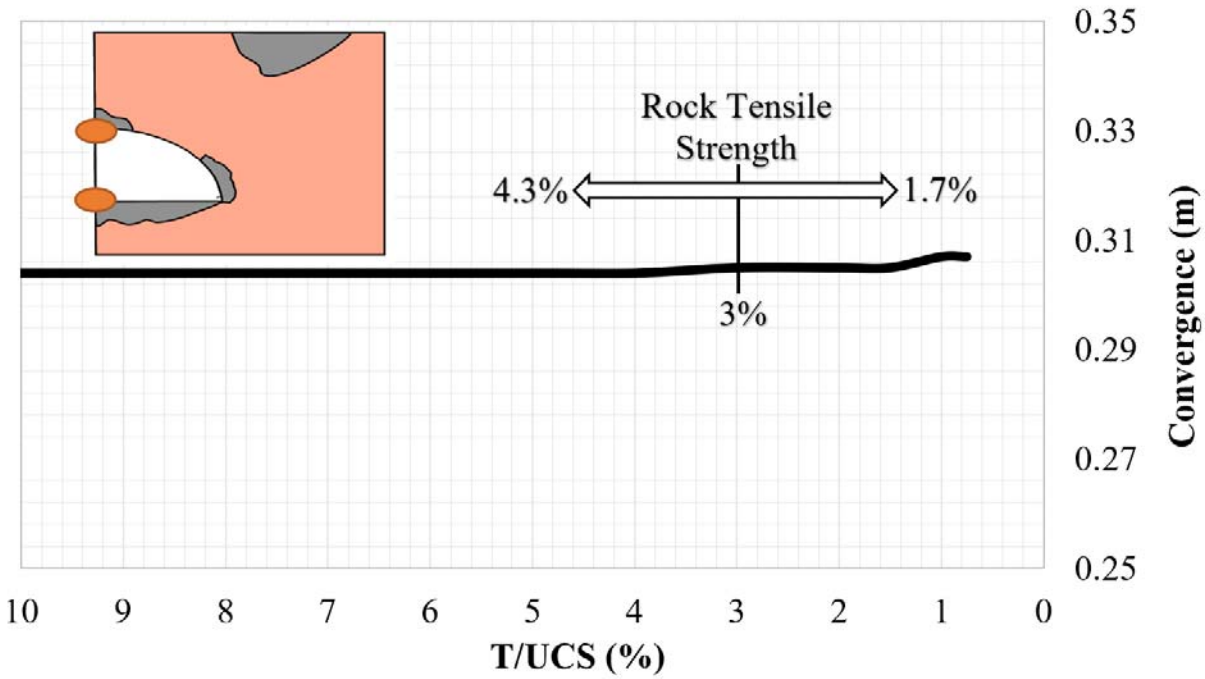

Fig.8. Tunnel convergence for the lava tube 1,000 m wide and 500 m roof thickness.

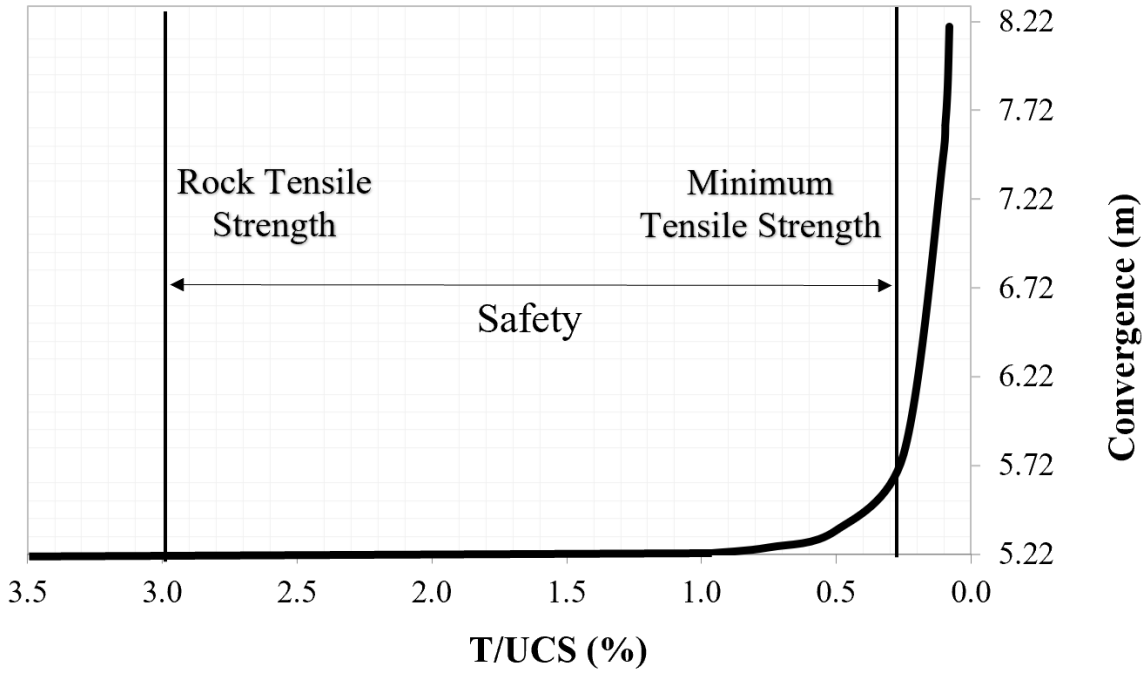

Fig.9. Tunnel convergence for the lava tube 4,000 m wide and 2,000 m roof thickness.

Table 4 compares the stability of the lava tubes analyzed based on the two criteria discussed. The results indicate that lava tubes on the Moon are likely to be stable with sizes of 1-4 km in width, given that the rock is moderately fractured such that it retains capacity in tension and has adequate overburden.

Table 4. Stability of lava tubes using the yielding height (h/H%) and the convergence (m).

Criterion	Width=4,000 m, Roof thickness= 2,000 m	Width=1,000 m, Roof thickness= 500 m
Yielding Height (h/H%)	Quasi-Stable	Stable
Convergence (m)	Stable	Stable

IV. Conclusions

The results of an analytical solution presented in this paper support the GRAIL observations that indicate the existence of large vacant substructures under the surface of the Moon. Geological and mechanical considerations concerning the formation of the lava tubes indicate that sizes of the lava tubes of about 1 km are possible, which supports estimates from GRAIL data. Lava tubes with this size could provide potential habitats for astronauts on the Moon.

Previous numerical simulations showed that lava tubes as large as 4 km wide could remain stable with a roof thickness as small as ~40 m. More realistic assumptions regarding the tensile capacity of the overburden rock indicate that larger roof thicknesses might be necessary for the lava tubes to remain stable or, conversely, a small overburden or small capacity of the rock in tension may require smaller sizes of the lave tubes to remain stable.

V. References

[1] Maghareh, A., et al. (2018) *LPSC 49, 2083.*
[2] Dyke S. J., et al. (2018) *LPSC 49, 2882.*

[3] Hörz, F. (1985) *In: Mendell, W.W. (Ed.), Lunar Bases and Space Activities of the 21st Century (A86-3011,13-14). Lunar and Planetary Institute, Houston, TX,* 405–412.
[4] Haruyama, J., et al. (2012) *In: Badescu, V. (Ed.), Moon: Prospective Energy and Material Resources. Springer, Heidelberg, Germany*, 139–163.
[5] Coombs, C., Hawke, B. (1992) *In: Mendell, W.W. (Ed.), Lunar Bases and Space Activities of the 21st Century (31661). Lunar and Planetary Institute, Houston, TX,* 219-229.
[6] Cruikshank, D., Wood, C. (1971) *The moon 3, 412-447.*
[7] Sauro, F., et al. (2018) *LPSC 49, 2083.*
[8] Greeley, R. (1971) *The moon 3, 289-314.*
[9] Haruyama, J., et al. (2009) *GRL 36*, L21206.
[10] Haruyama, J., et al. (2010), *LPSC 41*, 1285.
[11] Robinson, M. S., et al. (2012) *Planet. Space. Sci. 69*, 18–27.
[12] Chappaz, L., et al. (2014a) *LPSC 45*, 1746.
[13] Chappaz, L., et al. (2014b) *AIAA Space 2014 Conf. and Expo.*, 4371.
[14] Sood R., et al (2017), *Icarus 289, 157-172.*
[15] Sood R., et al (2016b), *AIAA 26th Space Flight Mechanics Meetings.*
[16] Zuber et al. (2013), *Science 339, 668-671.*
[17] Lemoine et al. (2014), *GRL 41 (10), 3382-3389.*
[18] Oberbeck, V. R., et al. (1969) *Mod. Geol. 1*, 75–80.
[19] Blair D.M., et al. (2017) *Icarus 282*, 47-55.
[20] ABAQUS, Inc. (2017). ABAQUS V.6.16 user's manual, Providence, R.I.
[21] Kaku, T., et al. (2017), *GRL 44*, 10155-10161
[22] Melosh, H.J. (2011) *Cambridge University Press*.
[23] Moore, H.J., et al. (1978) *LPSC 9th*, 3351-3378.
[24] Hurwitz, D.M., et al. (2013) *Planetary and Space Science 79-80*, 1-38.
[25] Cashman, K.V., et al. (2006) *Bull Volcanol 68*, 753-770.
[26] Modiriasari et al. (2018) *LPSC 49, 2803.*
[27] Hoek, E., Brown, E., (1997) *International journal of rock mechanics and mining sciences*, 34.8 (1997): 1165-1186.
[28] Kiefer, W., et al. (2012), *GRL 39,* L07201.